

Noether symmetries in Interacting Quintessence Cosmology

Ester Piedipalumbo^{a,b,*}, Mariafelicia De Laurentis^{a,b,c}, Salvatore Capozziello^{a,b,d,e}

^a*Dipartimento di Fisica, Università degli Studi di Napoli Federico II, Compl. Univ. Monte S. Angelo,
80126 Naples, Italy*

^b*I.N.F.N., Sez. di Napoli, Compl. Univ. Monte S. Angelo, Edificio 6, via Cinthia, 80126 - Napoli, Italy*

^c*Lab. Theor. Cosmology, Tomsk State University of Control Systems and Radioelectronics (TUSUR), 634050
Tomsk, Russia*

^d*Gran Sasso Science Institute, Viale F. Crispi, 7, I-67100, L'Aquila, Italy*

^e*Tomsk State Pedagogical University, ul. Kievskaya, 60, 634061 Tomsk, Russia*

Abstract

The Noether Symmetry Approach is applied to interacting quintessence cosmology with the aim to search for exact solutions and select scalar-field self-interaction potentials. It turns out that the solutions found are compatible with the accelerated expansion of the Universe and with observational dataset, as the SNeIa Pantheon data.

Keywords: Modified gravity; cosmology; Noether symmetries; exact solutions.

1. Introduction

Over the last decades, observational data revealed that the present Universe is experiencing an accelerated expansion driven by the so-called dark energy [44, 45, 52, 53]. Dark energy was first revealed observationally by examining the light from distant type Ia supernovae [40, 41]. Actually, it turned out that a new form of energy (with negative pressure) is needed to accelerate the Hubble flow. According to recent estimates, dark energy provides about 70% of the total amount of matter-energy in the Universe, and only 5% of the Universe is constituted by standard elements we (*i.e.* protons, neutrons, electrons, photons, neutrinos, and even gravitational waves). The remaining 25% is constituted by dark matter. The nature of dark energy and dark matter is yet unknown, and, despite many proposals, both of them escape a final understanding at fundamental level. So far, some of the proposed models to account for dark energy include non-vanishing cosmological constant, potential energy of some scalar fields, effects connected to inhomogeneous distributions of matter and averaging procedures, and effects due to alternative/extended theories of gravity [2, 12, 17, 24, 26, 36–38, 43].

*Corresponding author

Email addresses: ester@na.infn.it (Ester Piedipalumbo), felicia@na.infn.it (Mariafelicia De Laurentis), capozziello@na.infn.it (Salvatore Capozziello)

In particular, among these last theories, there are the scalar-tensor theories of gravity that includes both scalar fields and tensor fields to represent gravitational interaction [30]. These theories arise in fundamental contexts like, for example, low-energy limits of Kaluza-Klein theories, string gravity or quantum field theory formulated in curved spacetimes [5, 17, 39]. Furthermore, they have been widely investigated in both early- and late-universe expansions [27, 35, 48]. Recently, it has been suggested that such scalar fields are not fundamental but they might consist of fermion condensates [13, 54]. There are also other possibilities listed and discussed, for example, in [3]. Actually, the dynamical dark energy models have their own issues, as the cosmic coincidence problem, *i.e.*, the circumstance that dark energy and dark matter are, today, of the same order of magnitude even if they evolve independently. Non-gravitational interactions between dark matter and dark energy has been recently proposed to avoid such an issue. Interacting dark matter/dark energy models have been studied in different contexts [1, 3, 8–11, 20–24, 31, 33, 34, 51, 55]. However, the form of the interaction between dark matter and dark energy is not known, and there is an arbitrary freedom to choose any specific interaction model.

This paper is aimed to understand whether this coupling can be connected to some symmetry. Specifically, by the so called *Noether Symmetry Approach*, it is possible to select suitable forms of interactions and scalar field potentials capable of addressing the dark matter/dark energy issue in the cosmological expansion.

In Section 2, we search for the existence of Noether symmetries to the point-like Lagrangian describing a single scalar field cosmological model coupled to dark matter. We show that the existence of symmetry allows a coupled dark energy field and provides an explicit form for the self-interaction potential leading the dark matter-dark energy interaction. In Section 3, we derive general exact solutions which naturally give rise to accelerated behaviors. Section 4 is devoted to compare the theoretical solutions with observations using the publicly available Pantheon SNeIa dataset. In Section 5 we draw conclusions.

2. Noether symmetries for interacting quintessence

The Noether Symmetry Approach is a useful tool to find out exact solutions, in particular in cosmology, and select conserved quantities [4, 14–16, 18, 19, 25, 28, 49, 50]. The existence of Noether symmetry allows to reduce the dynamical system that, in most cases, results integrable. It is interesting to note that the self-interacting scalar-field potentials, [14, 16, 28], the couplings [14, 28], or the overall structure of the theory [15], can be related to the existence of the symmetries (*i.e.* the conserved quantities). In this sense, the Noether Symmetry Approach is also a criterion to select reliable models (see [15, 29] for a discussion).

In the present case, let us consider a 4-dimensional gravitational action where a quintessential, minimally coupled scalar field interacts with the dark matter component:

$$\mathcal{A} = \int d^4x \sqrt{-g} \left[\frac{1}{2}R + \frac{1}{2}g^{\mu\nu} \phi_{;\mu;\nu} - V(\phi) + \tilde{\mathcal{L}}_m(g_{\mu\nu}, \phi) \right], \quad (1)$$

where g is the determinant of the metric tensor $g_{\mu\nu}$ while $V(\phi)$ is the self-interaction

potential of the scalar field ϕ . Furthermore, we consider

$$\tilde{\mathcal{L}}_m(g_{\mu\nu}, \phi) = \mathcal{L}_m(g_{\mu\nu}) + \mathcal{L}_m^{int}(g_{\mu\nu}, \phi), \quad (2)$$

where $\mathcal{L}_m(g_{\mu\nu})$ is the standard matter Lagrangian term and $\mathcal{L}_m^{int}(g_{\mu\nu}, \phi)$ is the interaction term. We are using physical units ($G_N = c = \hbar = 1$).

2.1. Cosmological equations

Assuming a spatially flat Friedmann-Robertson-Walker cosmology, with metric signature $(-, +, +, +)$, the resulting point-like Lagrangian, derived from Eq.(1), can be written as

$$\mathcal{L} = 3a\dot{a}^2 - a^3 \left(\frac{\dot{\phi}^2}{2} - V(\phi) \right) + Ma^{-3(\gamma-1)} + Ma^{-3(\gamma-1)}F(a, \phi), \quad (3)$$

where $a = a(t)$ is the scale factor of the Universe, and the constant M is related to the today matter density ρ_m^0 , where $1 \leq \gamma \leq 2$. The term $Ma^{-3(\gamma-1)}F(a, \phi)$ describes the interaction between the dark matter-dark energy components. Here, the dot represents the derivative with respect to the cosmic time t . In the following, we will limit our analysis to $\gamma = 1$, corresponding to the dust case. Due to the presence of the interaction term in the Lagrangian, the dark-matter energy density no longer evolves simply as a^{-3} but instead scales as

$$\rho_{\text{DM}} \sim \frac{1 + F(a, \phi)}{a^3}. \quad (4)$$

It is possible to redefine $F(a, \phi)$ in order to absorb all terms, including the potential $V(\phi)$, into a single function:

$$F(a, \phi) \rightarrow \tilde{F}(a, \phi) = a^3V(\phi) + Ma^{-3(\gamma-1)}(1 + F(a, \phi)). \quad (5)$$

This choice has no effect in the search for Noether symmetries and the results are the same with only a single function being involved. However, the form used in the action (3) offers the advantage to highlight contributions from different terms (scalar field potential, matter etc.). With these considerations in mind, the Friedmann equations are:

$$3H^2 = \frac{1}{2}\dot{\phi}^2 + V(\phi) + \frac{M}{a^3}(1 + F(a, \phi)), \quad (6)$$

$$2\left(\frac{\ddot{a}}{a}\right) + H^2 + \frac{1}{2}\dot{\phi}^2 - V(\phi) - \frac{M}{a^2}\frac{\partial F(a, \phi)}{\partial a} = 0, \quad (7)$$

$$\ddot{\phi} + 3H\dot{\phi} = -\frac{dV(\phi)}{d\phi} - \frac{M}{a^3}\frac{\partial F(a, \phi)}{\partial \phi}. \quad (8)$$

Eq.(8) for the scalar field is a generalized Klein-Gordon equation, and differs from the usual one by the last term, due to the interaction with the dark matter. If we want to find a *standard* form of the acceleration equation Eq.(7) as:

$$6\left(\frac{\ddot{a}}{a}\right) = -(\rho_{eff} + 3p_{eff}), \quad (9)$$

then an effective pressure of the ϕ -field is given by

$$p_\phi^{eff} = \frac{1}{2}\dot{\phi}^2 - V(\phi) + \frac{M}{3a^2} \frac{\partial F(a, \phi)}{\partial a}. \quad (10)$$

Analogously, it is possible to define an effective energy density of the scalar field by comparing Eq.(6) with its *standard* form:

$$3H^2 = \rho_m + \rho_\phi. \quad (11)$$

It turns out that

$$\rho_\phi^{eff} = \rho_\phi + Ma^{-3}F(a, \phi), \quad (12)$$

where ρ_ϕ is the standard term:

$$\rho_\phi = \frac{1}{2}\dot{\phi}^2 + V(\phi). \quad (13)$$

These two expressions define an effective equation of state

$$w_\phi^{eff} = \frac{p_\phi}{\rho_\phi} = \frac{\frac{1}{2}\dot{\phi}^2 - V(\phi) + \frac{M}{3a^2} \frac{\partial F(a, \phi)}{\partial a}}{\frac{1}{2}\dot{\phi}^2 + V(\phi) + Ma^{-3}F(a, \phi)}, \quad (14)$$

which drives the time behavior of the model.

2.2. The Noether Symmetry Approach

In order to derive an analytical form for the self-interaction potential $V(\phi)$ and for the dark matter- dark energy coupling $F(a, \phi)$, we proceed as follows, relying upon the work in Refs. [14, 28]. Given the point Lagrangian in Eq.(3), the configuration space is $\mathcal{Q} \equiv \{a, \phi\}$, while the tangent bundle is $T\mathcal{Q} \equiv \{a, \phi, \dot{a}, \dot{\phi}\}$. We look for point symmetries which are transformations on the tangent space $T\mathcal{Q}$ derived from transformations on the base space \mathcal{Q} . The infinitesimal generator of a point transformation reads as

$$X = \alpha \frac{\partial}{\partial a} + \beta \frac{\partial}{\partial \phi} + \frac{d\alpha}{dt} \frac{\partial}{\partial \dot{a}} + \frac{d\beta}{dt} \frac{\partial}{\partial \dot{\phi}}, \quad (15)$$

where

$$\frac{d\alpha}{dt} = \dot{\alpha} = \frac{\partial \alpha}{\partial a} \dot{a} + \frac{\partial \alpha}{\partial \phi} \dot{\phi}, \quad (16)$$

$$\frac{d\beta}{dt} = \dot{\beta} = \frac{\partial \beta}{\partial a} \dot{a} + \frac{\partial \beta}{\partial \phi} \dot{\phi}. \quad (17)$$

Here α and β are functions of $a(t), \phi(t)$. The vector field X on $T\mathcal{Q}$ is the complete lift [14] of the vector field on \mathcal{Q}

$$Y = \alpha \frac{\partial}{\partial a} + \beta \frac{\partial}{\partial \phi}. \quad (18)$$

The unknown functions α and β are determined by requiring that the Lie derivative along X of the point Lagrangian \mathcal{L} is vanishing, *i.e.*

$$L_X \mathcal{L} = X \mathcal{L} = \alpha \frac{\partial \mathcal{L}}{\partial a} + \beta \frac{\partial \mathcal{L}}{\partial \phi} + \frac{d\alpha}{dt} \frac{\partial \mathcal{L}}{\partial \dot{a}} + \frac{d\beta}{dt} \frac{\partial \mathcal{L}}{\partial \dot{\phi}} = 0. \quad (19)$$

This means that the Lagrangian is conserved along the flow generated by the vector field X , *i.e.* Eq.(19) holds all over the tangent bundle of the configuration space. According to (15)-(17), Eq. (19) takes the form

$$\begin{aligned} & 3\dot{a}^2 \left(\alpha + 2a \frac{\partial \alpha}{\partial a} \right) - \dot{\phi}^2 \frac{a^2}{2} \left(3\alpha + 2a \frac{\partial \beta}{\partial \phi} \right) \\ & + \dot{a} \dot{\phi} a \left(6 \frac{\partial \alpha}{\partial \phi} - a^2 \frac{\partial \beta}{\partial a} \right) \\ & + \left[3\alpha a^2 V(\phi) + \alpha M \frac{\partial F}{\partial a} + \beta \left(a^3 V'(\phi) + M \frac{\partial F}{\partial \phi} \right) \right] = 0. \end{aligned} \quad (20)$$

For this equation to be satisfied, the terms in round and square brackets must vanish separately, which yields the system of first-order partial differential equations

$$\alpha + 2a \frac{\partial \alpha}{\partial a} = 0, \quad (21)$$

$$3\alpha + 2a \frac{\partial \beta}{\partial \phi} = 0, \quad (22)$$

$$6 \frac{\partial \alpha}{\partial \phi} - a^2 \frac{\partial \beta}{\partial a} = 0, \quad (23)$$

$$\left[3\alpha a^2 V(\phi) + \alpha M \frac{\partial F}{\partial a} + \beta \left(a^3 V'(\phi) + M \frac{\partial F}{\partial \phi} \right) \right] = 0. \quad (24)$$

Here the prime indicates the derivative with respect to the scalar field ϕ . Eqs. (21)-(23) can be solved by the factorized ansatz

$$\alpha(a, \phi) = A_1(a)B_1(\phi), \quad \beta(a, \phi) = A_2(a)B_2(\phi). \quad (25)$$

Eq. (21) becomes then a first-order ordinary differential equation for $A_1(a)$, which is solved by

$$A_1(a) = \frac{1}{\sqrt{a}}, \quad (26)$$

up to a multiplicative constant, and hence Eqs. (22) and (23) lead to

$$A_2(a) \frac{dB_2}{d\phi} = -\frac{3}{2} a^{-\frac{3}{2}} B_1(\phi), \quad (27)$$

$$\frac{dA_2}{da} B_2(\phi) = 6a^{-\frac{5}{2}} \frac{dB_1}{d\phi}. \quad (28)$$

Therefore, we obtain

$$A_2(a) = \kappa a^{-\frac{3}{2}}, \quad (29)$$

$$\frac{dB_1}{d\phi} = -\frac{\kappa}{4}B_2(\phi), \quad \frac{dB_2}{d\phi} = -\frac{3}{2\kappa}B_1(\phi), \quad (30)$$

where κ is a constant. This leads to a second-order equation for $B_2(\phi)$, from which we get

$$\alpha = \frac{Ae^{\frac{1}{2}\sqrt{\frac{3}{2}}\phi} + Be^{-\frac{1}{2}\sqrt{\frac{3}{2}}\phi}}{\sqrt{a}}, \quad (31)$$

$$\beta = \frac{\sqrt{6}e^{-\frac{1}{2}\sqrt{\frac{3}{2}}\phi} \left(B - Ae^{\sqrt{\frac{3}{2}}\phi} \right)}{a^{3/2}}, \quad (32)$$

where the value $a = 0$ has to be excluded. We can choose $A = 0$ and solve Eq. (24) separating the part involving the potential $V(\phi)$ and its first derivative. We find:

$$V(\phi) = V_0 e^{-\sqrt{\frac{3}{2}}\phi}. \quad (33)$$

Therefore, the remaining symmetry condition implies that $F(a, \phi) = \mathcal{F}(\phi - 6 \ln a)$, that is \mathcal{F} is an arbitrary function of $(\phi - 6 \ln a)$. If we select $\mathcal{F} = e^{-\frac{k(\phi - \sqrt{6} \log(a))}{\sqrt{6}}}$ we find, from (24),

$$F(a, \phi) = Qa^k e^{-\frac{k\phi}{\sqrt{6}}}, \quad (34)$$

where V_0 and Q are constants. It is worth noticing that, in this way, the Noether symmetry selects the self-interaction potential and coupling which are often assumed in literature for phenomenological reasons [6–10, 23]. It turns out that the solution in Eq. (34) can be recovered if we factorize

$$F(a, \phi) = F_1(a)F_2(\phi). \quad (35)$$

Moreover, for $k = 0$, we recover a quintessence scalar field with the exponential self-interaction potential. It is worth noticing that the other branch, $B = 0$, leads again to infinite possibilities, being $F(a, \phi) = \mathcal{F}(\phi + 6 \ln a)$ an arbitrary function. In the general case, when both $A, B \neq 0$, it is:

$$V(\phi) = e^{-\sqrt{\frac{3}{2}}\phi} V_0 \left(B - Ae^{\sqrt{\frac{3}{2}}\phi} \right)^2, \quad (36)$$

and

$$F(a, \phi) = \mathcal{F} \left(\phi - \sqrt{\frac{2}{3}} \left(3 \log(a) + 2 \log \left(B - Ae^{\sqrt{\frac{3}{2}}\phi} \right) \right) \right) \quad (37)$$

where the term in parentheses of $F(a, \phi)$ indicates an arbitrary function of its argument.

In the following, we limit our analysis to the solution given in Eqs. (33) and (34) which reproduce potentials and coupling used in literature, for which we can find exact solutions of the cosmological equations.

3. Exact cosmological solutions

Once the infinitesimal generator X is found, it is possible to find a change of variables $\{a, \phi\} \rightarrow \{u, v\}$, such that one of them (say v , for example) is cyclic for the Lagrangian \mathcal{L} in Eq. (3), and the transformed Lagrangian produces, in general, solvable equations. Integrating the system of equations $i_X du = 0$ and $i_X dv = 1$ (where $i_X du$ and $i_X dv$ are the contractions between the vector field X and the differential forms du and dv , respectively), we obtain

$$a = (uv)^{\frac{1}{3}}, \quad (38)$$

$$\phi = -\sqrt{\frac{2}{3}} \log \left[\frac{u}{v} \right]. \quad (39)$$

Under this transformation, the Lagrangian takes the form

$$\mathcal{L} = M + MQu^{\frac{2k}{3}} + V_0 u^2 + \frac{4\dot{v}\dot{u}}{3}, \quad (40)$$

where v is cyclic. The conserved current gives

$$\Sigma = \frac{\partial \mathcal{L}}{\partial \dot{v}} = \frac{4}{3} \dot{u}, \quad (41)$$

which can be trivially integrated to obtain

$$u = \frac{3}{4} \Sigma t + u_0. \quad (42)$$

The energy condition $E_{\mathcal{L}} = 0$ has been used to find v . It is easy to show that the variable v satisfies the following differential equation:

$$\dot{v} - \frac{V_0}{\Sigma} \left(u_0 + \frac{3\Sigma}{4} t \right)^2 - \frac{M}{\Sigma} \left[1 + Q \left(u_0 + \frac{3\Sigma}{4} t \right)^{\frac{2k}{3}} \right] = 0. \quad (43)$$

It is

$$v = \frac{2^{-\frac{4}{3}(k+3)}}{9(2k+3)\Sigma^2} \times \left[144MQ(3\Sigma t + 4u_0)^{\frac{2k}{3}+1} + 2^{4k/3}(2k+3) \left(144\Sigma(Mt + \Sigma v_0) + V_0(3\Sigma t + 4u_0)^3 \right) \right]. \quad (44)$$

The substitution of the function u in Eq. (38), and the solution v of the Eq.(39), provides the explicit forms of scale factor and scalar field. A family of solutions, parametrized by k , are found. In the next Section, we will discuss some special values of k . In order to obtain $v(t)$, we can solve Eq. (39) after substituting the value for k , or, alternatively, start from Eq. (44), and specify the value k . It follows, that the two solutions differ for a constant. In the next Subsection we will discuss some special cases.

3.1. The case $k = -3$

Let us consider the special case $k = -3$. Eqs.(42) and (43) read as

$$u = \frac{3}{4}\Sigma t + u_0, \quad (45)$$

$$v = -\frac{16MQ}{9\Sigma^3 t + 12\Sigma^2 u_0} + \frac{Mt}{\Sigma} + \frac{V_0(3\Sigma t + 4u_0)^3}{144\Sigma^2} + v_0. \quad (46)$$

In order to obtain the scale factor $a(t)$, and the scalar field $\phi(t)$, we set $v_0 = 0$, and consider some constraints among the integration constants. For this purpose we impose the condition $a(0) = 0$, and we set the present time at $t_0 = 1$. This fixes the time-scale according to the age of the Universe. Because of our choice, the expansion rate $H(t)$ is dimensionless, so that our Hubble constant $\hat{H}_0 = H(t_0)$ is clearly of order 1 and not (numerically) the same as the H_0 that is usually measured in $\text{kms}^{-1}\text{Mpc}^{-1}$. Actually, \hat{H}_0 fixes only the product $h\tau$, and depends on the integration constants. Therefore, it is possible to *constrain* their range of variability, starting from \hat{H}_0 . We then set $a_0 = a(1) = 1$, and $\hat{H}_0 = H(1)$.

By means of these choices and of the formulae in Eqs. (A.1) and (A.2), we can construct all relevant cosmological parameters: $\rho_\phi, p_\phi, V_\phi, w_\phi, \rho^{eff}, p^{eff}$, and w^{eff} . As it is shown in Fig.(1), our model allows an accelerated expansion as indicated from the observations and exhibits an evolving equation of state, as shown in Fig. (2), where we compare the effective equation of state, w_{eff} , and the scalar field w_ϕ . Furthermore, in Fig.(3), we present the plot $\log \rho - \log(1+z)$ compared with different matter-energy densities. Moreover, no violation of the weak energy condition is observed.

In Fig. (4), we plot the distance modulus for fixed values of H_0, u_0 and Σ , compared with that one predicted in the standard ΛCDM model.

3.2. The cases $k = \frac{3}{2}$ and $k = 3$.

Another interesting solution is for $k = \frac{3}{2}$. Also in this case we start from Eqs. (42) and (43), so that

$$u = \frac{3}{4}\Sigma t + u_0, \quad (47)$$

$$v = \frac{24M \left(\frac{1}{4}Q(3\Sigma t + 4u_0)^2 + 6\Sigma t \right) + V_0(3\Sigma t + 4u_0)^3 + 144\Sigma^2 v_0}{144\Sigma^2}$$

We then fix $v_0 = 0, a_0 = a(1) = 1$, and $\hat{H}_0 = H(1)$ to get some constraints among the integration constants. The scale factor and the scalar fields are in Appendix.

As it is shown in Fig. (5), also this solution allows for an accelerated expansion, and exhibits an evolving equation of state. In Fig. (6), we compare the effective equation of state, w_{eff} , and that of scalar field w_ϕ . Finally, we present the plot $\log \rho - \log(1+z)$ compared with different energy densities (7). In particular, for $k = 3$, setting $u_0 = 0, Q = \Sigma = 1$, we recover the special case of a minimally coupled scalar field with the exponential potential already analyzed in [19, 22, 42]. The scale factor, and the scalar

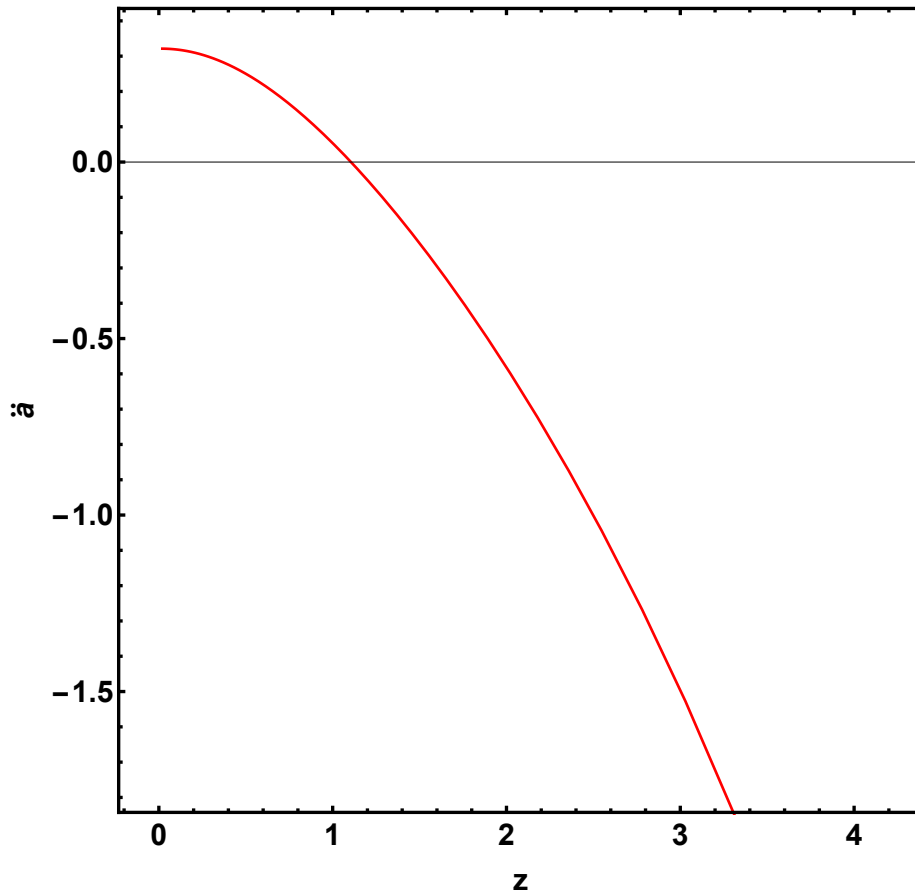


Figure 1: The case $k = -3$: redshift dependence of the acceleration $\ddot{a}(t)$: we see that the model allows for an accelerated phase of expansion, as indicated by the observations.

field are given in (A.5) and (A.6) (see Appendix). Also this solution corresponds to an accelerated expansion of the Universe, and exhibits an evolving equation of state, as shown in Fig. (8).

4. Comparing with observations

In order to investigate the reliability of this class of models, we present a comparison of theoretical predictions with the most updated compilation of SNeIa given in the Pantheon survey [52]. Our preliminary analysis is limited to the $k = 3$ model.

4.1. Data sample and statistical analysis

The SNeIa sample consists of 1048 objects in the range $0.01 < z < 2.26$. This sample is a combination of 365 spectroscopically confirmed SNeIa discovered by the

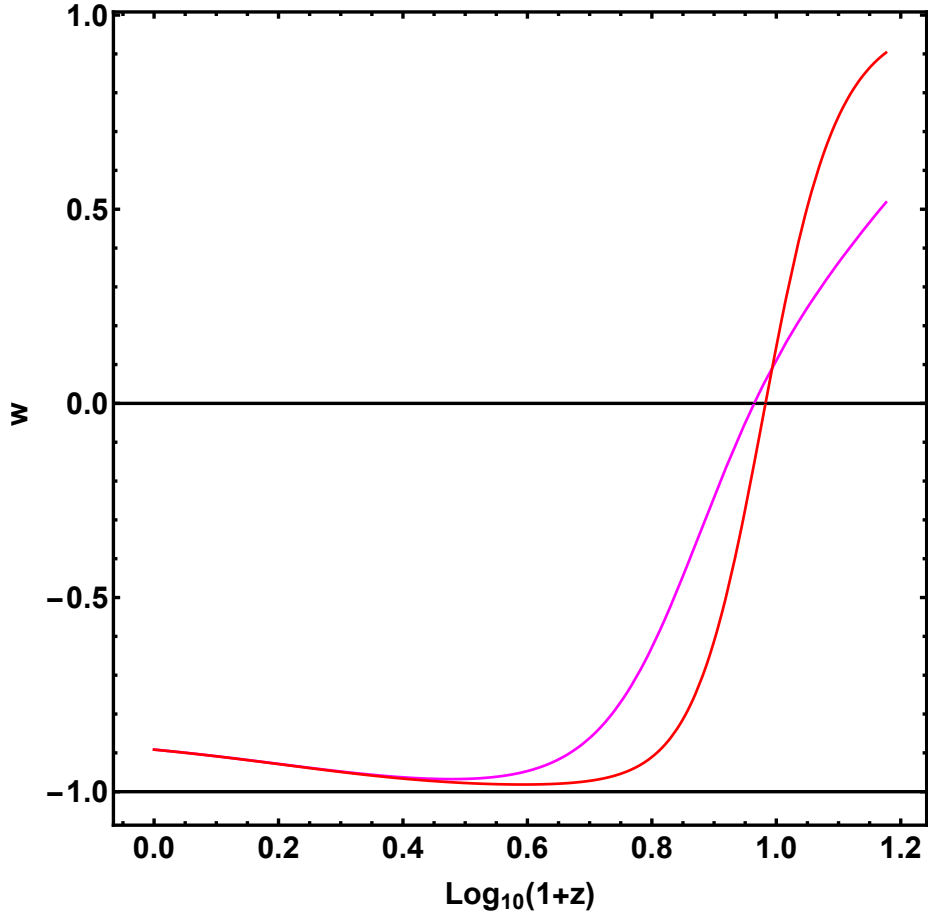


Figure 2: The case $k=-3$: redshift dependence of the equation of state parameter w_{eff} (red line) and w_ϕ (magenta line) for fixed value of H_0 , u_0 , and Σ .

Pan-STARRS1 PS1 Medium Deep Survey together to the subset of 279 PS1 SNeIa in the range ($0.03 < z < 0.68$) with distance estimates from SDSS, SNLS, various low redshift and HST samples. See [52] for details on photometry, astrometry, calibration, and systematic uncertainties. The SNeIa observations provide the apparent magnitude $m(z)$ at the peak luminosity after several corrections. The resulting apparent magnitude $m(z)$ can be easily related to the Hubble free luminosity distance through the relation:

$$m_{th}(z) = \bar{M} + 5 \log_{10}(D_L(z)). \quad (48)$$

Here \bar{M} is the zero point offset and depends on the absolute magnitude M and on the present value of the Hubble parameter. The cosmological model parameters can be

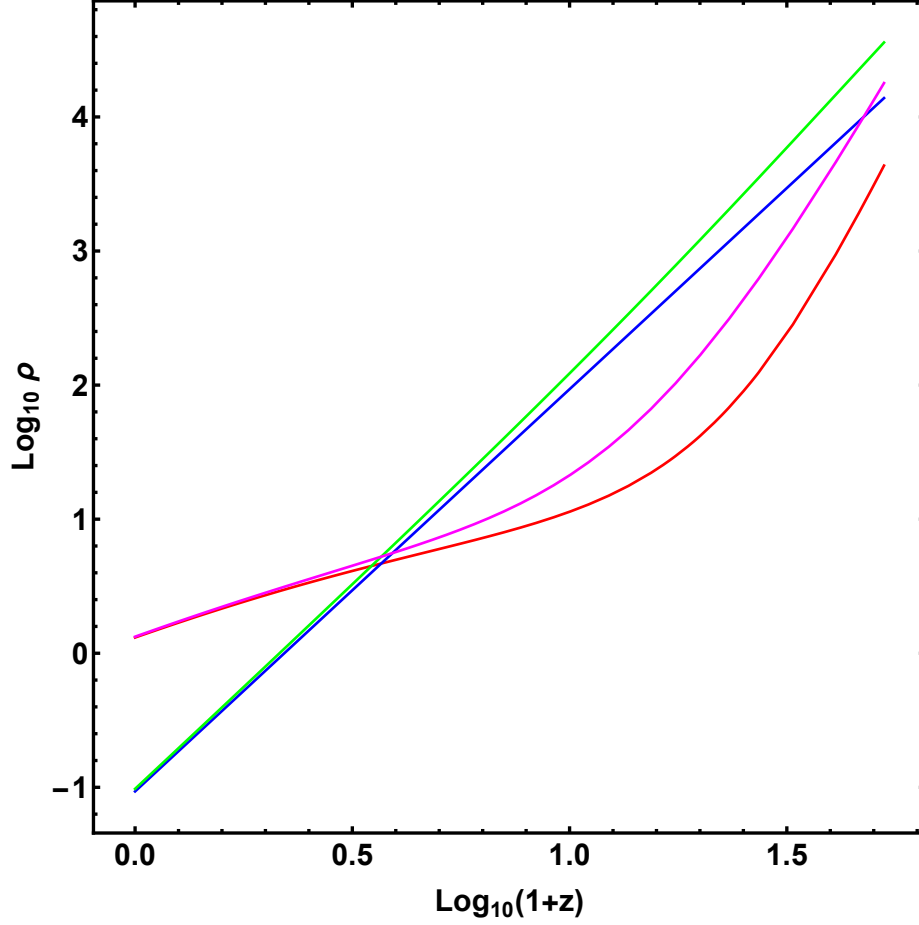


Figure 3: The case $k = -3$: plot of $\log_{10} \rho$ versus $\log_{10} 1 + z$ for fixed values of H_0 , u_0 and Σ . The blue line indicates the log-log plot of $\log_{10} \bar{\rho}_m \propto \log_{10} a^{-3}$, the green line is the dark matter density $\rho_{\text{DM}} \sim \frac{1 + Q_1(a)Q_2(\phi)}{a^3}$, the red and magenta lines correspond to ρ_ϕ and ρ_{eff} respectively, according to the Eqs.(12) and (13).

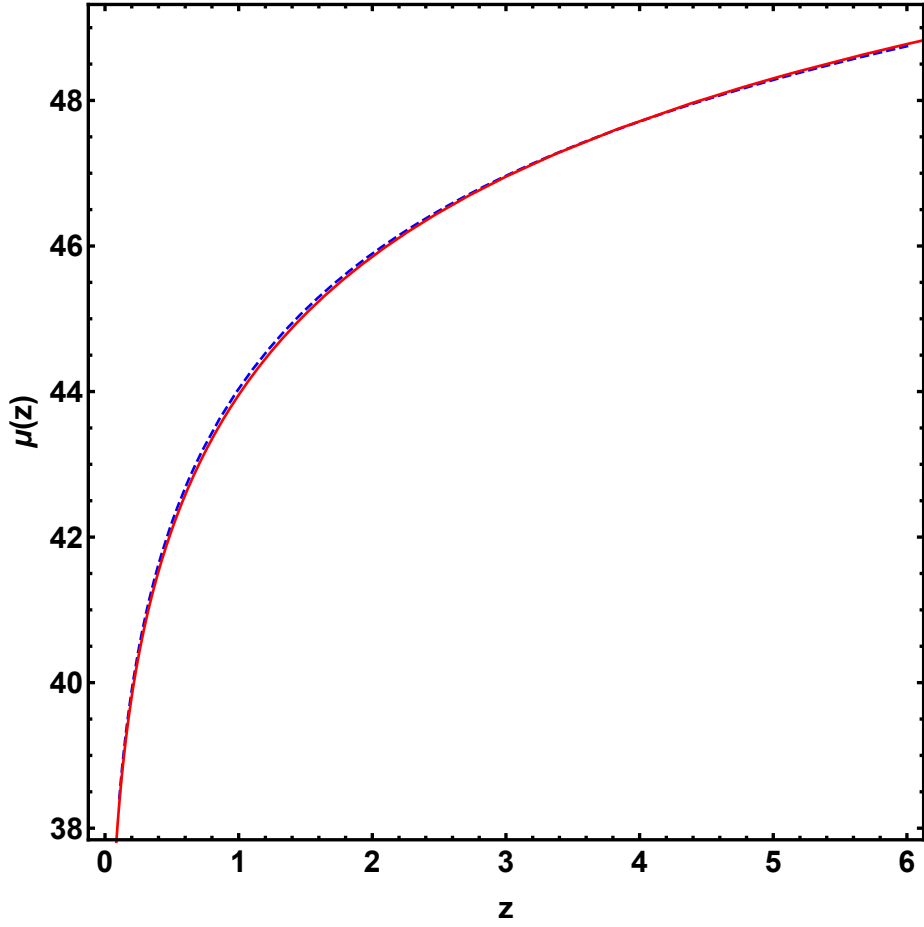


Figure 4: The case $k = -3$: distance modulus for fixed values of H_0, u_0 (red solid line), compared with that one predicted in the standard Λ CDM model (blue dashed line).

determined by minimizing the quantity

$$\chi_{SNIa}^2(\{\theta_p\}) = \sum_{i=1}^N \frac{(\mu_{obs}(z_i) - \mu_{th}(z_i, \{\theta_i\}))^2}{\sigma_{\mu i}^2}. \quad (49)$$

The theoretical distance modulus is therefore defined as

$$\mu_{th}(z_i, \{\theta_p\}) = 5 \log_{10}(D_L(z_i, \{\theta_p\})) + \nu_0, \quad (50)$$

where D_L is the luminosity distance:

$$D_L = \frac{c}{100h} (1+z) \int_0^z \frac{1}{H(\zeta, \theta)} d\zeta. \quad (51)$$

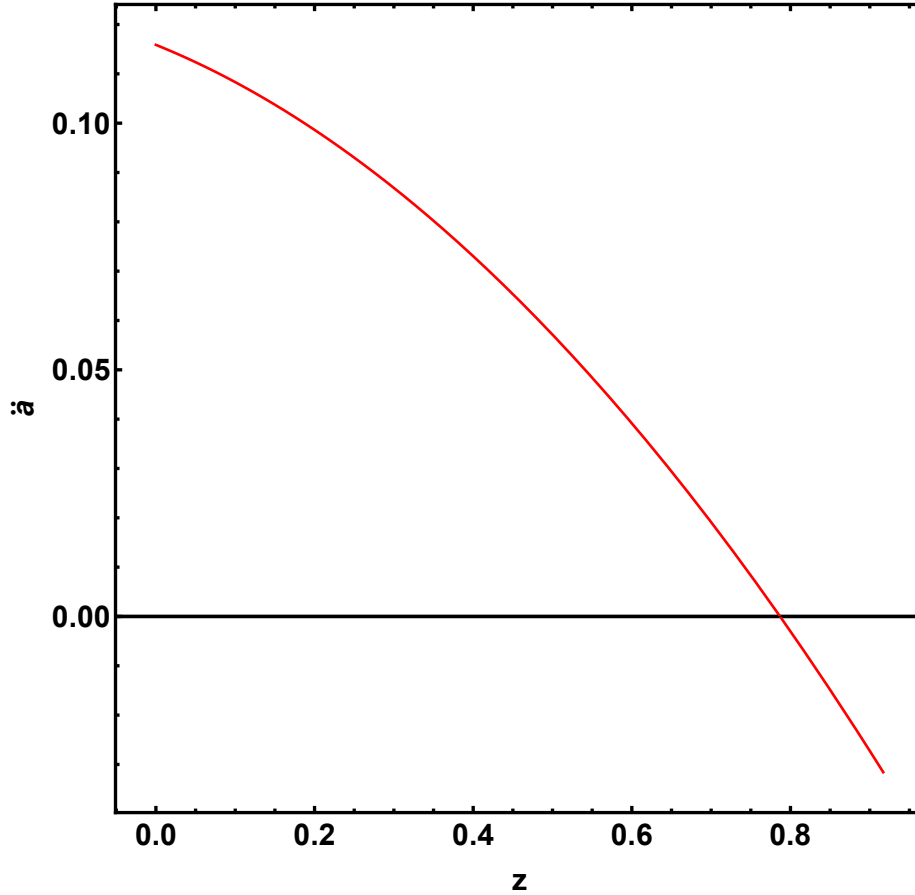


Figure 5: The case $k = \frac{3}{2}$: redshift dependence of the acceleration $\ddot{a}(t)$: we see that also this model allows for an accelerated phase of expansion, as indicated by the observations.

The parameter ν_0 encodes the Hubble constant. The absolute magnitude M and $\{\theta_p\}$ are model parameters. Actually, it is well known that using only SNeIa, one cannot constrain the Hubble constant, without including measurements of its local value from the SHOES project [46, 47], since this is degenerate with M . In order to set the starting points for our chains, we first perform a preliminary and standard fitting procedure to maximize the likelihood function $\mathcal{L}(\mathbf{p})$:

$$\mathcal{L}(\mathbf{p}) \propto \frac{\exp(-\chi_{SNIa}^2/2)}{(2\pi)^{\frac{N_{SNIa}}{2}} |\mathbf{C}_{SNIa/GRB}|^{1/2}}. \quad (52)$$

To build up their own regions of confidence, we use the Bayesian approach based on the Markov Chain Monte Carlo (MCMC) method. According to this procedure, we run three parallel chains and use the Gelman - Rubin diagnostic approach to test the convergence. We discard the first 30% of the point iterations at the beginning of any

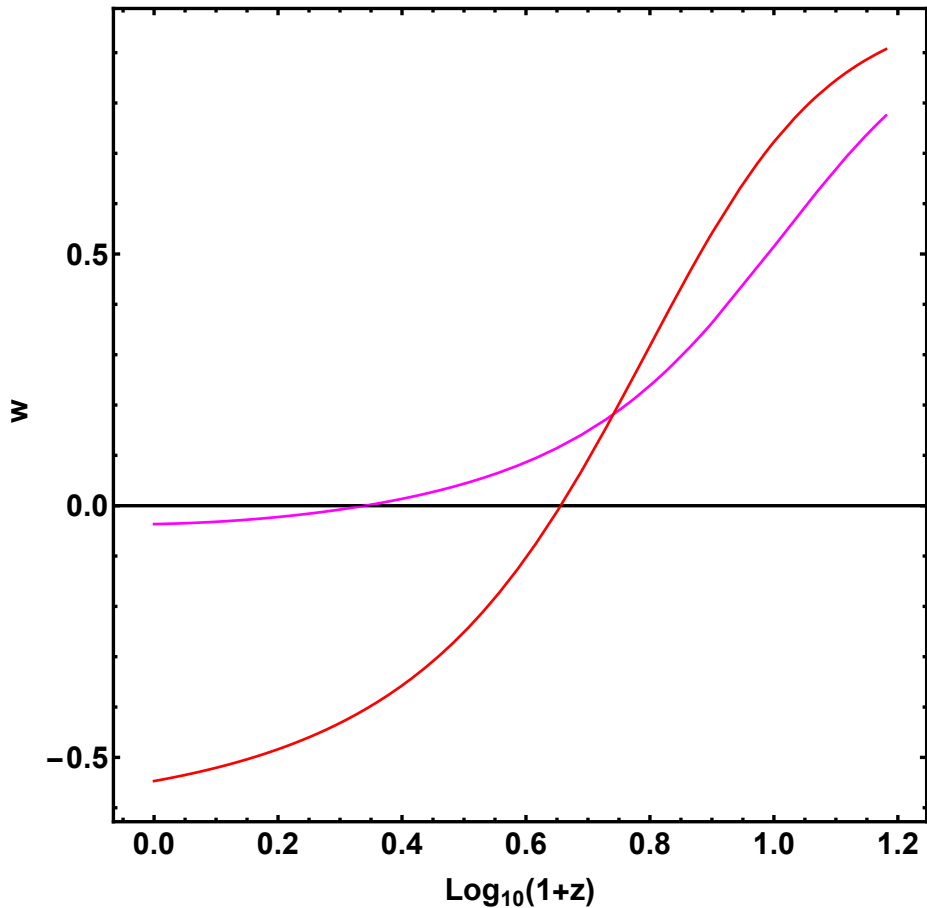


Figure 6: The case $k = \frac{3}{2}$: redshift dependence of the equation of state parameter w_{eff} (red line) and w_ϕ (magenta line) for fixed value of H_0 , u_0 , and Σ .

MCMC run, and then the chains that have to be run many times. We finally extract the constraints on the parameters by co-adding the thinned chains. It turns out that $H_0 = 0.98 \pm 0.07$, $u_0 = 0.23 \pm 0.09$, and $\Sigma = 1.1 \pm 0.2$. In Fig. (9), we plot the best fit curve with superimposed data set.

5. Discussion and Conclusions

In this paper, we investigated the possibility that coupled quintessence dynamics could be derived from the Noether Symmetry Approach. The method allows to select both the self-interacting potential of the scalar field and the analytical form of the interaction. We recover the exponential function widely used in literature, just confirming that the existence of the Noether symmetries offers a physical criterion to fix potentials, couplings and, in general, the form of models. Such an approach revealed extremely

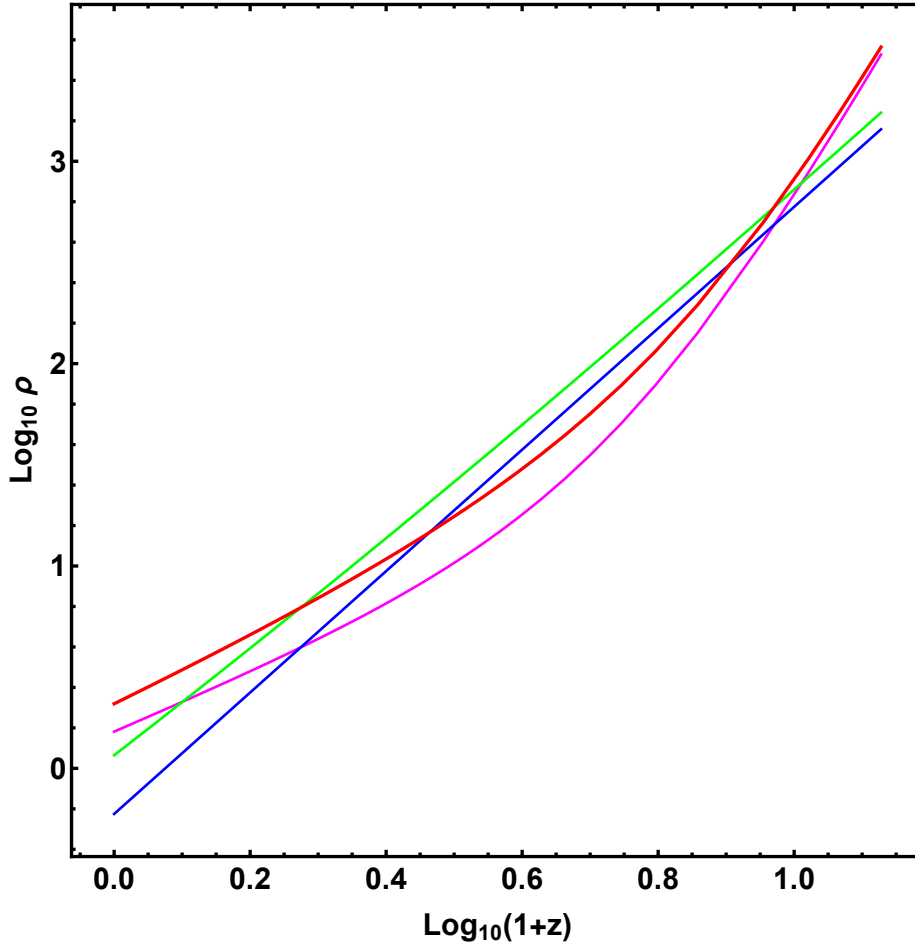


Figure 7: $k = \frac{3}{2}$: plot of $\log_{10} \rho$ versus $\log_{10}(1+z)$ for fixed values of H_0 , u_0 and Σ in the $k = \frac{3}{2}$. As in the previous subsection the blue line indicates the log-log plot of $\log_{10} \tilde{\rho}_m \propto \log_{10} a^{-3}$, the green line is the dark matter energy density $\rho_{DM} \sim \frac{1 + Q_1(a)Q_2(\phi)}{a^3}$, the red and magenta lines correspond to ρ_ϕ and ρ_{eff} respectively, according to the Eqs. (12) and (13).

useful also for other classes of models [14, 16, 18]. Moreover, by this approach, we are able to solve exactly the Friedmann equations, at least in the case of dark energy and matter dominated Universe. Specifically, we obtain a one-parameter family of exact solutions. The main cosmological observables can be directly derived starting from the general solutions. In order to match the results with observations, we consider a special value of the parameter k , and compared the theoretical solution with observational dataset using Pantheon data on SNeIa. It turns out, that the model is quite well compatible with this SNeIa data set. In forthcoming paper, we will discuss solutions coming from Noether symmetries with different datasets in order to achieve a reliable

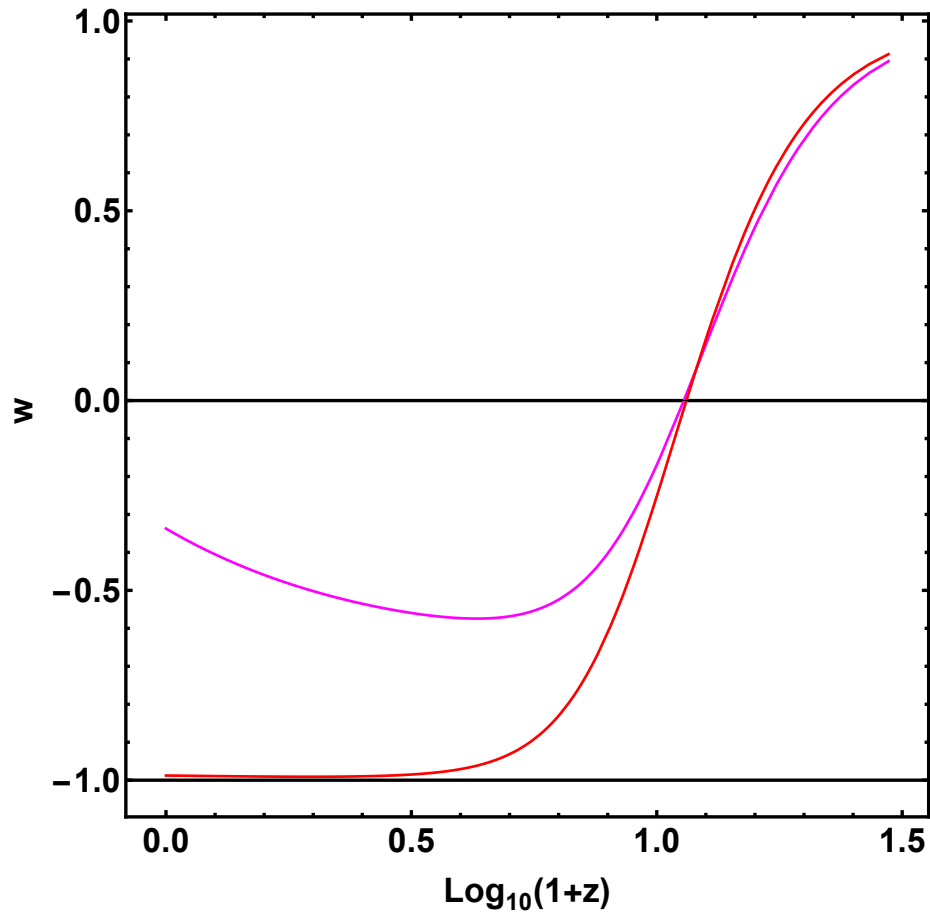


Figure 8: The case $k = 3$: redshift dependence of the equation of state parameter w_{eff} (red line) and w_ϕ (magenta line) for fixed value of H_0 , and Σ .

cosmic history at different redshifts.

Acknowledgements

We acknowledge INFN Sez. di Napoli (*Iniziativa Specifiche* MOONLIGHT2, QGSKY and TEONGRAV). This article is based upon work from COST Action CA15117 Cosmology and Astrophysics Network for Theoretical Advances and Training Actions (CANTATA), supported by COST (European Cooperation in Science and Technology). We acknowledge the anonymous referee for her/his suggestions that allowed to improve the manuscript.

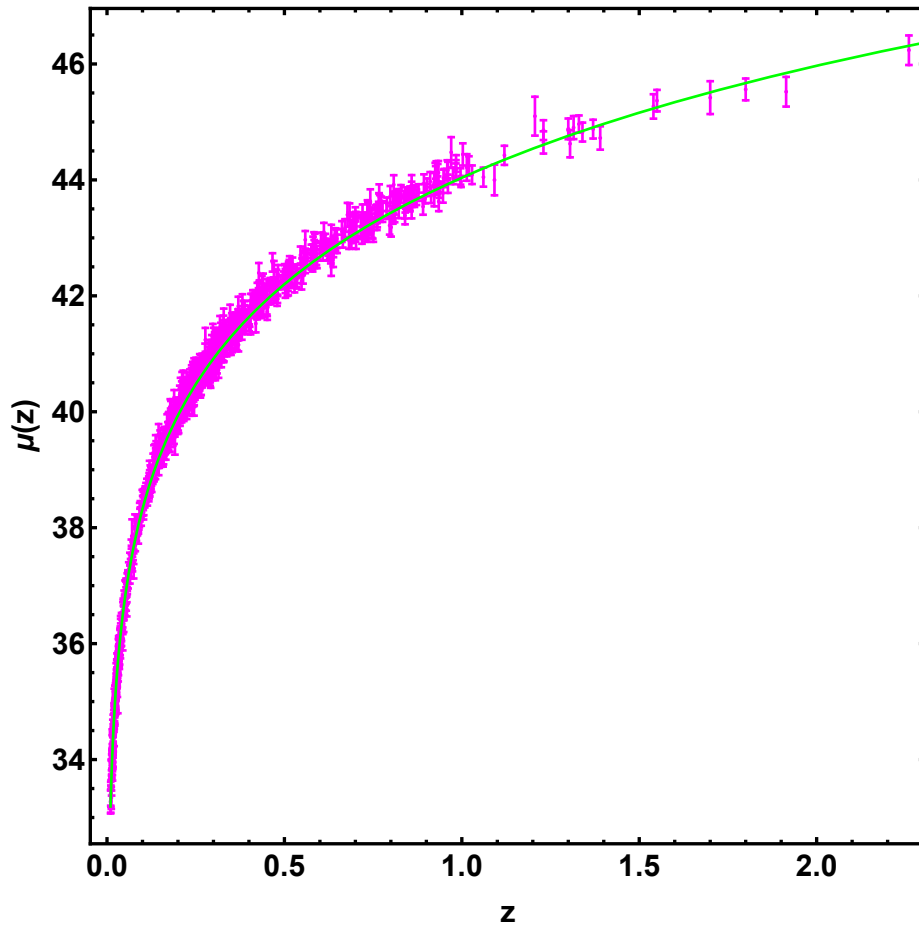


Figure 9: Comparison between the observational Pantheon data and the theoretical distance modulus (green line) for the model $k = \frac{3}{2}$, corresponding to the best fit values for the parameters.

References

- [1] L. Amendola, Phys. Rev. D **62**, 043511 (2000); L. Amendola and D. Tocchini-Valentini, Phys. Rev. D **64**, 043509 (2001); L. Amendola, C. Quercellini, D. Tocchini-Valentini and A. Pasqui, Astrophys. J. **583**, L53 (2003); L. Amendola and C. Quercellini, Phys. Rev. D **68**, 023514 (2003); G. Olivares, F. Atrio-Barandela and D. Pavon, Phys. Rev. D **71**, 063523 (2005); Amendola, L., Appleby, S., Avgoustidis, A. et al. Living Rev Relativity (2018) 21: 2.
- [2] R. Arona, W Cardona, S. Nesseris, Phys. Rev. D **99** (2019) 043516
- [3] S. Bahamonde, C. Boehmer, G. Christian, S. Carloni, E.J. Copeland, W. Fang, N. Tamanini, 2018, Physics Reports, **775**, 1-122

- [4] S. Basilakos, S. Capozziello, M. De Laurentis, A. Paliathanasis and M. Tsamparlis, *Phys. Rev. D* **88** (2013) 103526
- [5] N.D.Birrell, and P.C.W.Davies, *Quantum fields in curved space*, Cambridge University Press, **7**, (1984).
- [6] C.G. Boehmer, N. Tamanini, and M. Wright, 2015, *Phys. Rev. D* **91**, 123003
- [7] C.G. Boehmer, N. Tamanini, and M. Wright, 2015, *Phys. Rev. D* **91**, 123002
- [8] S.A. Bonometto, M. Mezzetti, R. Mainini, 2017, *JCAP*, **10**, 011
- [9] S.A. Bonometto, R. Mainini, M. Mezzetti, 2019, *MNRAS*, **486**, 2321
- [10] D.. Boriero, S. Das, Yvonne Y. Y. Wong, 2015, *JCAP*, **07**, 33
- [11] P. Brax, C. van de Bruck, A.C. Davis, J. Khoury and A. Weltman, *Phys. Rev. D* **70**, 123518 (2004)
- [12] Y-F. Cai, S. Capozziello, M. De Laurentis, E. N. Saridakis *Rept. Prog. Phys.* **79** (2016) 106901.
- [13] S. Carloni, R. Cianci, P. Feola, E. Piedipalumbo, S. Vignolo, *JCAP* **09** (2019), 014.
- [14] S. Capozziello, R. de Ritis, C. Rubano, and P. Scudellaro, , *Riv. Nuovo Cim.* **19** (4), 1
- [15] S. Capozziello and A. De Felice, *JCAP* **0808** (2008) 016.
- [16] S. Capozziello, S. Nesseris, L. Perivolaropoulos, 2007, *JCAP* **0712**, 009
- [17] S. Capozziello and M. De Laurentis, *Phys. Rept.* **509** (2011) 167
- [18] S. Capozziello, M. De Laurentis and S. D. Odintsov, *Mod. Phys. Lett. A* **29** (2014) no.30, 1450164
- [19] S. Capozziello, E. Piedipalumbo, C. Rubano, P. Scudellaro, *Astronomy & Astrophysics*, **505**, 21 (2008).
- [20] S. Capozziello, R. D'Agostino, O. Luongo, *I.J.Mod.Phys. D* **28**, 1930016 (2019).
- [21] T. Damour, G.W. Gibbons and C. Gundlach, *Phys. Rev. Lett.* **64**, 123 (1990); J.A. Casas, J. Garcia-Bellido and M. Quiros, 1992, *Clas. Quant. Grav.* **9**, 1371; R. Bean, 2001, *Phys. Rev. D* **64**, 123516; D. Comelli, M. Pietroni and A. Riotto, 2003, *Phys. Lett. B* **571**, 115; U. Franca and R. Rosenfeld, 2004, *Phys. Rev. D* **69**, 063517 (2004); L. P. Chimento, A. S. Jakubi, D. Pavon and W. Zimdahl, 2003, *Phys. Rev. D* **67**, 083513
- [22] M. Demianski, C. Rubano, C. Tortora, 2005, *Astron.Astrophys.* **431**, 27-43

- [23] S. Das, P. Corasaniti and J. Khoury, 2006, Phys. Rev.D **73**, 083509
- [24] M. Demianski, E. Piedipalumbo, C. Rubano, C. Tortora, 2006, Astron.Astrophys., **454**, 55-66
- [25] M. Demianski, E. Piedipalumbo, C. Rubano, P. Scudellaro, 2008, Astron. & Astrophys., **481**, 279
- [26] M. Demianski, E. Piedipalumbo, D. Sawant, L. Amati, Astronomy & Astrophysics, **598**, (2017b) A113
- [27] M. Demianski & E. Piedipalumbo, Eur.Phys.J. C, **79** (2019), 575
- [28] R. de Ritis, G. Marmo, G. Platania, C. Rubano, P. Scudellaro, and C. Stornaiolo, 1990, Phys. Rev. D **42**, 1091
- [29] K. F. Dialektopoulos and S. Capozziello, Int. J. Geom. Meth. Mod. Phys. **15** (2018), 1840007
- [30] V. Faraoni, *Cosmology in Scalar-tensor Gravity*, Fundamental Theories of Physics, Ed. Springer, Dordrecht (2011).
- [31] G.R. Farrar and P.J.E. Peebles, 2004, Astrophys. J. **604**, 1; S.S. Gubser and P.J.E. Peebles, 2004, Phys. Rev. D**70**, 123510
- [32] R. Hagala, Llinares C., Mota D.F., 2016, Astronomy & Astrophysics, **585**
- [33] D.B. Kaplan, A.E. Nelson and N. Weiner, 2004, Phys. Rev. Lett. **93**, 091801; R. D. Peccei, 2005, Phys. Rev. D**71**, 023527
- [34] J. Khoury and A. Weltman, 2004, Phys. Rev. Lett. **93**, 172204; J. Khoury and A. Weltman, 2004, Phys. Rev. D **69**, 044026; S.S. Gubser and J. Khoury, 2004, Phys. Rev. D **70**, 104001.
- [35] A.Joyce, L.Lombriser,F.Schmidt, 2016, Annual Review of Nuclear and Particle Science,**66**, 95-122
- [36] S. Nesseris, D. Sapone, S. Sypas, Phys.Dark Univ. **27**, (2020) 100413
- [37] S. Nojiri and S. D. Odintsov, Phys. Rept. **505** (2011) 59
- [38] S. Nojiri, S. D. Odintsov and V. K. Oikonomou, Phys. Rept. **692** (2017) 1
- [39] J. M. Overduin and P. S. Wesson. Kaluza-Klein Gravity. Phys. Rept. **283**, 303 (1997).
- [40] S. M. Perlmutter, G. Aldering, M. Della Valle, S. Deustua, R.S. Ellis, R. S., et al, Nature, **391**, (1998) 51
- [41] S. M. Perlmutter, G. Aldering, . G. Goldhaber, R. Knop, P. Nugent, et al., ApJ, **517**, (1999) 565

- [42] E. Piedipalumbo, P. Scudellaro, G. Esposito, 2012, *General Relativity and Gravitation*, **44**, 2611
- [43] E. Piedipalumbo, E. Della Moglie, R. Cianci, *Int. J. of Mod. Phys. D*, **24**, (2015) 1550100
- [44] Planck Collaboration, 2016, *Astronomy & Astrophysics*, **594**, A13
- [45] A.G. Riess, L.G. Strolger, S. Casertano, H.C. Ferguson, B. Mobasher, et al., 2007, *ApJ*, **659**, 98
- [46] A.G. Riess, L. Macri, W. Li, H. Lampeitl, S. Casertano, et al., *ApJ*, **699**, (1999) 539
- [47] A.G. Riess, L.M. Macri, S.L. Hoffmann, D., Scolnic, S. Casertano, et al., *ApJ*, **826**, (2016)56R
- [48] B. Saha, 2015, *Astrophys. Space Sci.* **357**, 28.
- [49] A. K. Sanyal, C. Rubano, and E. Piedipalumbo, *Gen. Rel. and Grav.*, **35**, (2003) 1617
- [50] A. K. Sanyal, B. Modak, C. Rubano, and E. Piedipalumbo, *Gen. Rel. and Grav.*, **37**, (2005) 407
- [51] A.K. Sanyal, *IJMP A*, 2007, **22**, 1301
- [52] D. M. Scolnic, D.O. Jones, A. Rest, et al. 2018, *ApJ*, **859**, 101
- [53] Suzuki et al. (The Supernova Cosmology Project), *ApJ*, **46**, (2012) 85
- [54] S. Vignolo, S. Carloni and L. Fabbri, 2015, *Phys. Rev. D* **91**, 043528.
- [55] H. Wei and R. G. Cai, 2005, *Phys. Rev. D* **71**, 043504

Appendix A. Cosmological solutions for the cases $k = -3, 3/2, 3$

In this Appendix we show the expressions for the scale factor and the scalar field corresponding to the cases we considered.

- $k = -3$. It is:

$$a(t)^3 = \frac{t(3\Sigma t + 8u_0)}{2(3\Sigma + 4u_0)(3\Sigma + 8u_0)^2} \times \\ [9\Sigma^2((3H_0 - 2)t^2 - 3H_0 + 4) + 24\Sigma u_0(3H_0(t^2 + t - 2) - t(t + 2) + 6) \\ + 64u_0^2(3H_0(t - 1) - t + 2)] , \quad (\text{A.1})$$

$$\exp \left[\sqrt{\frac{3}{2}} \phi(t) \right] = \frac{1}{(3\Sigma + 4u_0)(3\Sigma + 8u_0)^2(3\Sigma t + 4u_0)^2} \times \\ [8t(3\Sigma t + 8u_0)(3H_0(t - 1)(3\Sigma + 8u_0)(3\Sigma(t + 1) + 8u_0) \\ - 2(3\Sigma + 4u_0)(3\Sigma(t^2 - 2) + 8(t - 2)u_0))] . \quad (\text{A.2})$$

- $k = 3/2$. It is

$$a(t)^3 = \frac{1}{(3\Sigma + 4u_0)^2(3\Sigma^2 + 16\Sigma(u_0 + 1) + 16u_0(u_0 + 2))} \times \\ \{ t [27\Sigma^4 t^2(3H_0(t - 1) - 3t + 4) + 36\Sigma^3 t(3u_0 + 2)((3H_0 - 2)t^2 - 3H_0 + 4) \\ + 64\Sigma u_0^2(5u_0 + 8)(3H_0(t^2 - 1) - t^2 + 3) + 96\Sigma^2 u_0(3H_0(t - 1)(t((t + 4)u_0 + t + 5) + u_0 + 1) \\ + 4(3t + u_0 + 1) - t(t((t + 6)u_0 + t + 8) - 9u_0)) + 256u_0^3(u_0 + 2)(3H_0(t - 1) - t + 2)] \} , \quad (\text{A.3})$$

$$\exp \left[\sqrt{\frac{3}{2}} \phi(t) \right] = \frac{1}{(3\Sigma + 4u_0)^2(\Sigma(3\Sigma + 16) + 16u_0(\Sigma + u_0 + 2))(3\Sigma t + 4u_0)} \times \\ 16t[3H_0(t - 1)(3\Sigma + 4u_0)(\Sigma((3\Sigma + 8)t + 8) + 8u_0(\Sigma + \Sigma t + 2u_0 + 4)) \\ + 3\Sigma^2(-9\Sigma + 16)t^2 + 12\Sigma t + 32) + 4u_0(\Sigma(24(\Sigma + 4) - t(-9\Sigma + 2(9\Sigma + 4)t + 48)) \\ + 4u_0(15\Sigma - 2t(\Sigma(t + 3) + 4) - 4(t - 2)u_0 + 16))] . \quad (\text{A.4})$$

- $k = 3$. It is

$$a(t)^3 = \frac{t(3\Sigma t + 4u_0)}{2(\Sigma + 2u_0)(3\Sigma + 4u_0)^2} \times \\ 3\Sigma^2 [((3H_0 - 2)t^2 - 3H_0 + 4) + 4\Sigma u_0(3H_0(t - 1)(t + 4) \\ - t(t + 6) + 12) + 16u_0^2(3H_0(t - 1) - t + 2)] . \quad (\text{A.5})$$

$$\exp \left[\sqrt{\frac{3}{2}} \phi(t) \right] = \frac{8t}{(\Sigma + 2u_0)(3\Sigma + 4u_0)^2(3\Sigma t + 4u_0)} \times \\ [3\Sigma^2((3H_0 - 2)t^2 - 3H_0 + 4) + 4\Sigma u_0(3H_0(t - 1)(t + 4) - t(t + 6) + 12) \\ + 16u_0^2(3H_0(t - 1) - t + 2)] . \quad (\text{A.6})$$